Estimation of Discharge Coefficient in Orifice Meter by Computational Fluid Dynamics Simulation

Muslim Danesh and Ahmad M. Hassan

Department of Petroleum – Drilling and Refining, Kurdistan Technical Institute, Slemani Heights, Sulaimaniya, Kurdistan Region – Iraq

***Abstract*—Orifices are devices for measuring mass flow rates of liquids in pipes. The discharge coefficient is an important design characteristics of orifice. In this work, analysis of flow through an orifice is simulated using ANSYS Fluent computational fluid dynamics (CFD) software. Three cases with different ratios of orifice bore diameter to pipe diameter have been investigated. The discharge coefficient for each case was estimated, and the results have been compared to empirical correlation. The results show that, for installing an orifice, the suitable point should be selected for the location of pressure tapping. CFD was also used for the prediction of vena contracta after the orifice. It shows that the location of vena contracta is affected by the size of the orifice bore and can be determined from the velocity data.**

***Index Terms*—Computational fluid dynamics, Discharge coefficient, Orifice, Velocity.**

I. Introduction

An orifice meter comprises of an orifice plate, a holding device, downstream and upstream meter piping, and pressure taps. The orifice plate is placed between two flanges, which uses as holding system. The sharp-edge orifice is common because of its simplicity in design and financially (low cost). Furthermore, sizing of orifice relies on flow measurement criteria to be achieved. Three classes of problems involving orifices are: (1) Unknown pressure drop, (2) Unknown flow rate and (3) unknown orifice diameter. And each of these can be determined having known the other two parameters. For example, for design problems when the orifice diameters is unknown, the size is determined for a specified (maximum) flow rate of a given fluid in a given pipe with a pressure drop device that has a given (maximum) range.

For the purpose of flow measurement by an orifice, the accuracy of the discharge coefficient has greater importance. The discharge coefficient is a dimensionless number used to characterize the flow and pressure loss behavior of orifices in fluid systems. The discharge coefficient, C_d, varies considerably with changes in area ratio and the Reynolds number [1]. Finding the discharge coefficient of a specific orifice requires precise measurements. With the help of computational fluid dynamics (CFD), the task becomes easier. Tukiman *et al*. done a CFD simulation on the shape of velocity and pressure profile in orifices [2]. Other researches attempted to study the effect of orifice to pipe diameter by both CFD and experimental measurements [3,4].

A fluid system analysis by CFD comprises of solving partial differential equations (PDEs). For all practical purposes, the PDEs encountered cannot be solved explicitly. Rather a numerical solution of them is advantageous. CFD integrates the disciplines of fluid mechanics with mathematics and also computer science for the purpose of numerical solution of PDEs [5].

The governing equations that describe fluid systems represent mathematical statements of the conservation laws of physics, namely, conservation of mass, momentum, energy, and species [5].

The equation for conservation of mass, or continuity equation, can be written as follows [6]:

$$\frac{\partial \rho}{\partial t} + \nabla(\rho \vec{\upsilon}) = 0 \quad (1)$$

Conservation of momentum in an inertial (non-accelerating) reference frame is described by Navier–Stokes equations for Newtonian fluids [7]:

$$\frac{\partial}{\partial t}(\rho \vec{v}) + \nabla(\rho \vec{v}\vec{v}) = -\nabla p + \nabla(\vec{\tau}) + \rho \vec{g} + \vec{F} \quad (2)$$

Where $\vec{F}$ is the external force vector. The stress tensor is $\vec{\tau}$ given by:

$$\vec{\tau} = \mu\left[(\nabla\vec{\upsilon} + \nabla\vec{\upsilon}^{T}) - \frac{2}{3}\nabla\vec{\upsilon}\,\mathrm{I}\right] \quad (3)$$

For simple cases where the fluid is incompressible and energy and mass transfer is not important, these two equations are enough.

II. Problem Setup

Every CFD simulation is performed in four steps:

1. Pre-processing (creating geometry and generating the desired mesh).
2. Setting up the domain and boundary conditions.
3. Solving the PDE by discretizing.

Pure and Applied Science Conference | Koya University
Paper ID: ICPAS2018.REN44, 3 pages
DOI: 10.14500//icpas2018.ren44
Received 28 February 2018; Accepted 09 March 2018
Conference paper: Published 01 August 2018
Conference track: Renewable Energy (REN)
Corresponding author’s e-mail: muslim.amin@kti.edu.krd

4. Post-processing and analysis of results.

The geometry here is composed of a section of pipe with an orifice that was created using built-in ANSYS CAD software. The pipe is 0.1m in diameter. The length of the pipe was set sufficiently long to minimize the entrance effects. In many pipe flows of practical engineering interest, the entrance effects become insignificant beyond a pipe length of 10 diameters, and the hydrodynamic entry length is approximated as follows [8]:

$$L_{h,turbulent}=4.4Re^{\frac{1}{6}}D \quad (4)$$

Therefore, to ensure fully turbulent flow just before the orifice, the pipe was considered 5.0m long and the orifice plate was centered at the pipe. The investigation involves simulation of three different sizes of concentric orifice with bore diameters, *d*, equal to 0.03 m, 0.04 m, and 0.05 m (Fig. 1).

CFD requires the subdivision of the domain into a number of smaller, non-overlapping subdomains to solve the flow physics within the domain geometry that has been created [5]. The generated mesh is shown in Fig. 2.

The next step in CFD simulation is setting up the solver. The steady state solver is activated for the problem described here. Since almost all technical flows are turbulent, a suitable model to represent the turbulence should be selected. Averaging procedures are widely applied to the Navier–Stokes equations with RANS as the most used method. However, the averaging process introduces additional unknown terms into the transport equations (Reynolds Stresses and Fluxes) that need to be provided by suitable turbulence models (turbulence closures) [7].

The k-epsilon turbulent model is a two-equation model with standard wall treatment and is applied here for turbulent modeling in the flow domain.

The effect of gravity was also inserted into the model by setting gravitational acceleration equal to −9.81 m^2/s in the negative y-direction.

The flowing fluid through the pipe is water with constant properties of density $\rho=998.2\frac{kg}{m^a}$ and dynamics viscosity $\mu=1.003\times10-3\frac{kg}{m^s}$. Water enters the pipe with a uniform velocity of $0.2\frac{m}{s}$ from the left side and exits on the right side to air with static gauge pressure of 0 Pa. It is worth mentioning that all pressures, here, are gauge pressure relative to the atmospheric pressure.

III. Results and Discussion

After the simulation converged, the solution was analyzed in post-processing step. To distinguish between each orifice size, a parameter called area ratio, β, is defined as the ratio of orifice bore diameter to pipe diameter:

$$\beta=\frac{d}{D} \quad (5)$$

For orifice plate installations, the discharge coefficient will vary depending on the location of the pressure

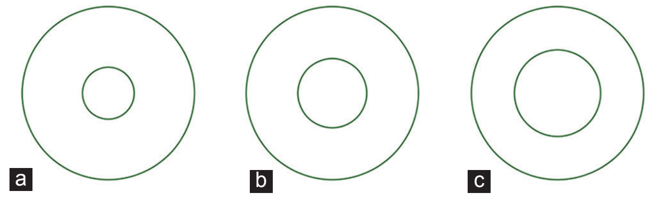

Fig. 1. Sharpe edge orifices with different bore diameter, d .
(a) d=0.03 m, (b) d=0.04 m, (c) d=0.05 m

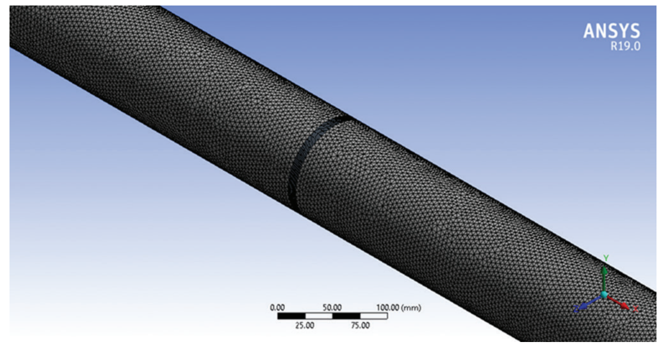

Fig. 2. A schematic of the pipe and orifice with generated mesh.

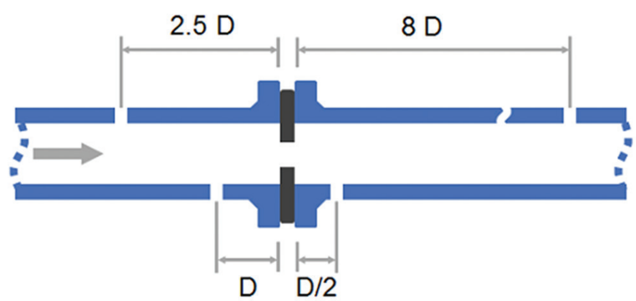

Fig. 3. Common pressure tapping locations in orifice installation.

tappings. Two common arrangements are tapping points at 2.5 pipe diameter upstream and 8 pipe diameter downstream (type 1) and tapping points at 1 pipe diameter upstream and half a pipe diameter downstream (type 2) as shown in the Fig. 3:

To calculate the discharge coefficient, C_d, the Bernoulli equation and mass conservation equation must be solved simultaneously:

$$m=\frac{C_d A_t}{\sqrt{1-A_t/A_1}}\sqrt{2\rho(P_1-P_2)} \quad (6)$$

Another way to find the discharge coefficient is by empirical correlation. The following correlations [9] are used for the validation of the CFD data for the calculation of discharge coefficients:

For tappings at 2.5D and 8D:

$$C_d = 0.5959+0.461\beta^{2.1}-0.480\beta^6+\frac{\rho VD}{\mu}=19904 \quad (7)$$

For tappings at 1D and 0.5D:

$$C_d = 0.5959+0.461\beta^{2.1}-0.184\beta^6\ \frac{0.039\beta^4}{1-\beta^4}-0.0158\beta^3+\frac{91.71\beta^{2.5}}{Re^{0.75}} \quad (8)$$

DOI: http://dx.doi.org/10.14500/icpas2018

TABLE I
DISCHARGE COEFFICIENT CALCULATED FROM THE CFD RESULT AND EMPIRICAL CORRELAITON

Variable	Orifice 1: β=0.3	Orifice 1: β=0.4	Orifice 1: β=0.5
Pressure at 2.5D upstream (Pa)	4087.98	1200.99	442.554
Pressure at 8D downstream (Pa)	12.9323	12.9658	12.8091
Pressure at 1D upstream (Pa)	4086.78	1199.81	441.384
Pressure at 0.5D downstream (Pa)	−417.805	−222.999	−130.375
Tapping at 2.5D and 8D			
Theoretical C_d	0.7056	0.6774	0.6473
Experimental C_d	0.6354	0.6678	0.7082
% error	11.048	1.44	8.6
Tapping at 1D and 0.5D			
Theoretical C_d	0.7419	0.7426	0.7466
Experimental C_d	0.6008	0.6053	0.6106
% error	23.48	22.68	22.27

TABLE II
COORDINATE, VELOCITY, AND PRESSURE AT VENA CONTRACTA POINT

β	Vena contracta coordinate	$u_{max}(\frac{m}{s})$	Pressure at VC (Pa)
0.3	[0.0102, −0.0006, 0.0007]	2.92524	−291.889
0.4	[0.0167, 0.0003, 0.0000]	1.67514	−186.721
0.5	[0.0308, 0.0018, 0.0020]	1.09111	−127.904

Where *Re* is the Reynolds number in both correlations and equal to:

$$Re=\frac{\rho VD}{\mu}=19904 \quad (9)$$

Table I summarizes the results for discharge coefficient of each orifice size.

It is evident from this table that increasing the orifice bore diameter, will increase the discharge coefficient. Furthermore, the value of discharge coefficient has less deviation from the correlation values when tappings are located at further distances of the orifice.

Another aspect of orifices is the vena contracta effect. By definition, vena contracta is the point where velocity reaches its maximum value. The coordinate of vena contracta, maximum velocity, and pressure at that point for three classes of orifices is shown in Table II.

The results show that the vena contracta point displaces further away from the orifice with increasing orifice bore diameter, as represented in Fig. 4.

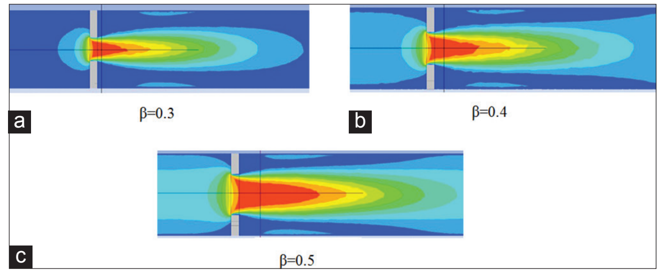

Fig. 4. (a-c) Vena contracta location (crossed lines) and contours of velocity around the orifice.

IV. CONCLUSION

Simulation is a powerful tool for predicting the flow behavior in industrial applications. Many designs, before a final product is emerged, should be studied by simulating them in a computer. This is to lower the cost of production, and on the other hand, to study the effect of many parameters that influence the performance of the product. Three sizes of orifice were investigated in this work, and the effect of size on discharge coefficient and vena contracta location was studied. Other factors such as the effect of pipe diameter, Reynolds number, fluid properties, and temperature effects could also be demonstrated by CFD modeling.

REFERENCES

[1] H. S. Bean, *Fluid Meters: Their Theory and Application: Report of ASME*. New York: American Society of Mechanical Engineers (ASME), 1971.

[2] M. M. Tukiman, M. N. M. Ghazali, A. Sadikin, N. F. Nasir, N. Nordin, A. Sapit and M. A. Razali, "CFD simulation of flow through an orifice plate," *IOP Conference Series: Materials Science and Engineering*, vol. 243, no. 1, 2017.

[3] F. Shan, Z. Liu, W. Liu and Y. Tsuji, "Effects of the orifice to pipe diameter ratio on orifice flows," Chemical Engineering Science, vol. 152, pp. 497-506, 2016.

[4] M. S. Shah, J. B. Joshi, A. S. Kalsi, C. S. R. Prasad and D. S. Shukla, "Analysis of flow through an orifice meter: CFD simulation," *Chemical Engineering* Science, vol. 71, pp. 300-309, 2012.

[5] J. Tu, G. Yeoh and C. Liu, *Computational Fluid Dynamics: A Practical Approach*, Oxford: Butterworth-Heinemann, 2007.

[6] R. B. Bird, W. E. Stewart and E. N. Lightfoot, *Transport Phenomena*, New York: J. Wiley, 2007.

[7] ANSYS, "*ANSYS Fluent Theory Guide*, Canonsburg: Ansys Inc, p. 848, 2018.

[8] Y. A. Çengel and J. M. Cimbala, F*luid Mechanics ecFundamentals and Applications*, New York: McGraw-Hill, 2006.

[9] P. J. LaNasa and E. L. Upp, *Fluid Flow Measurement: A Practical Guide to Accurate Flow Measurement*, 3rd ed. Oxford: Butterworth-Heinemann, 2014.